Available online at www.sciencedirect.com
SCIENCE DIRECT®
C. R. Mecanique 332 (2004) 181–187
COMPTES RENDUS MECANIQUE

Dynamics of irregularly shaped bodies in a flow behind a shock wave

V.M. Boiko, Sergey V. Poplavski

Institute of Theoretical and Applied Mechanics, Novosibirsk 630090, Russia

Received 9 July 2003; accepted after revision 21 November 2003

Presented by Évariste Sanchez-Palencia

Abstract

For the first time, the multi-frame shadow visualization technique coupled with a laser stroboscopic source of light has been used to obtain data on the dynamics of irregularly shaped bodies in the flow behind shock wave. A procedure for determining body acceleration from body trajectory is proposed, which, together with the diagnostic technique used, represents a kind of contactless aerodynamic balance. Drag data for spheres and irregularly shaped bodies in the flow behind shock wave with Mach number of 0.5 to 1.5 and Reynolds number of 10^5 are reported. ***To cite this article: V.M. Boiko, S.V. Poplavski, C. R. Mecanique 332 (2004).***

Résumé

La dynamique des corps de forme irrégulière dans un écoulement derrière une onde de choc. On a utilisé pour la première fois, la technique de visualisation en ombre multi-repère couplée avec une source de lumière laser stroboscopique afin d'obtenir des données sur la dynamique des corps solides irréguliers plongés dans un écoulement derrière une onde de choc. On propose une procédure originale pour déterminer l'accélération du corps à partir de sa trajectoire. Cette procédure, avec la technique du diagnostic utilisée, représente une sorte de balance aérodynamique évitant le contact. Les données sur la tirée pour des sphères et des corps de forme irrégulière ont été obtenues pour les écoulements derrière les ondes de choc correspondant aux nombres de Mach entre 0,5 et 1,5, et pour le nombre de Reynolds égal à 10^5. ***Pour citer cet article : V.M. Boiko, S.V. Poplavski, C. R. Mecanique 332 (2004).***

Keywords: Fluid mechanics; Non-laminar flows; Drag; Shock waves

Mots-clés : Mécanique des fluides ; Écoulements non-laminaires ; Tirée ; Ondes de choc

1. Introduction

Shock waves, the inevitable consequence of all explosion processes, display in two-phase media some specific features. For instance, the momentum transfer between the phases in the course of phase velocity relaxation is

E-mail address: s.poplav@itam.nsc.ru (S.V. Poplavski).

1631-0721/$ – see front matter
doi:10.1016/j.crme.2003.11.008

directly related with the aerodynamic properties of condensed-phase particles. The question in which measure the particle shape affects these properties is especially topical for phytogenic and mineral organic dusts since their particles are shaped as irregular crystals with a random number and shape of crystal faces. No experimental data on the drag of such particles were published in the literature. In reported numerical studies of two-phase flows, particles were assumed to be smooth spheres. The question to which extent this approximation is adequate to particular actual cases has not so far been addressed, nor did this question even arose since even for spherical particles no drag data for unsteady-flow conditions were reported.

In this connection, it is of interest to examine the dynamics of irregularly shaped bodies in the flow behind shock wave in the regimes characteristic of dust explosions, to determine their drag coefficient for a few model bodies taken as an example, and, comparing their dynamics with that of sphere, to reveal the effect of particle shape on their drag.

2. Experimental

In the present study, the dynamics of irregularly shaped particles was examined by the example of a $5 \times 5 \times 5$ mm cube. The choice of cubic shape (with its distinct edges and faces, typical of organic-dust particles) was motivated by the desire to have reproducible experimental conditions considering body shape. Nonetheless, even such a simple body displays a substantial from-test-to-test scatter in its dynamics depending on its initial orientation with respect to the direction of the flow. Fig. 1 shows two sets of pictures (the frames with even numbers follows at a time interval of 80 μsec) sampled from two picture sequences taken under identical shock-tube experimental conditions. In frames No 2, the traveling shock-wave front is clearly seen; both this front and the shock-induced flow move from left to right, causing the free bodies, a cube and a sphere, move in the same direction. In their initial stationary position, the bodies were spaced one and a half of the body size apart along the viewing direction in order to diminish their influence on each other.

In Fig. 1(a), the cube is oriented normally to the flow with one of its faces; nevertheless, in this case, its acceleration turned out to be lower compared to the cases in which the cube was oriented to the flow with one of its edges or one of its corners (Fig. 1(b)). The latter can be attributed to the fact that, in tests with various orientations, the aerodynamic force depended in a greater extent on the midsection area of the body than on its aerodynamic

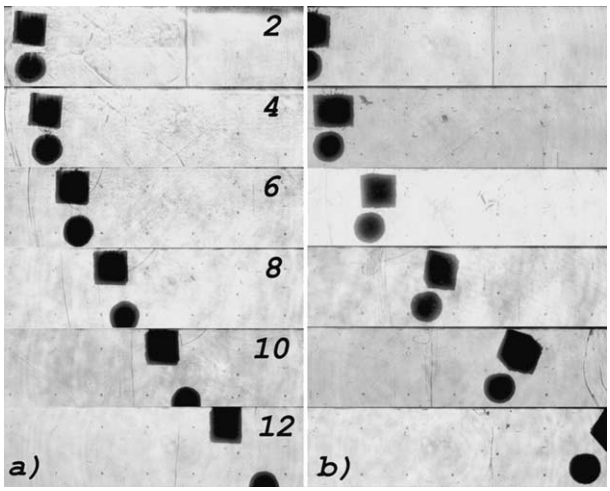

Fig. 1. Comparative dynamics of a cube and a sphere of identical sizes and densities for various orientations of the cube to the direction of the flow behind shock wave.

resistance. To run a few steps forward, note that the drag coefficient of the cube in case A ($C_x = 1.75$) was indeed greater than in case B ($C_x = 1.5$); however, the midsection areas in the two cases differed much greater, by the factor $\sqrt{3}$. Thus, the geometrical factor related with the rotation of irregularly shaped bodies in the flow exerts a greater influence on their translational motion than the aerodynamic one (for a cube, the corresponding ratio is $\approx 3/2$). The rotation of a body in a flow is observed more frequently than the specific behavior the cube displayed in case A; in the majority of cases, this rotation leads to establishment of some stable orientation of body relative to the flow velocity vector. Numerous observations showed that, for a cube, the most stable orientation is such in which the flow washes the cube approaching it parallel to its large diagonal.

Considering the substantial influence of initial orientation of the cube on its dynamics in the flow and with the aim to rule out possible influence of the second body, we performed a series of tests with isolated irregular bodies. Under conditions typical of the early development stage of dust explosions, namely, under unsteady-flow Mach number 0.5 to 1.5, we examined the drag coefficient C_x of freely accelerating irregular bodies; similar experiments with spheres were performed to obtain reference data for the same experimental conditions. In the present study, the following determination procedure for C_x was used. By definition, the drag coefficient C_x of a body is the ratio between the aerodynamic force F_a and the force due to the dynamic pressure acting upon the body midsection area s: $C_x = F_a/(s[\rho(u-V)^2/2])$ where ρ is the gas density, u and V are the flow and free body velocity. If the body mass m is known, then, instead of carrying out force measurements, it is possible to calculate the coefficient C_x from the acceleration A of the free body:

$$C_x = \frac{2mA}{s\rho(u-V)^2} = \frac{2m}{s\rho}\frac{1}{L} \tag{1}$$

where $L = (u-V)^2/A$ is a quantity, having the dimensions of length, to be experimentally determined from the flow velocity and the mean acceleration A of the body. This acceleration can be found with the help of multi-frame registration of body trajectories, taking into account that acceleration is doubly differentiated displacement. This approach became possible due to implementation of the multiple exposure shadowgraph technique coupled with a laser stroboscopic source of light and followed by subsequent processing of gained data on the body trajectory on a personal computer with the help of a special software complex.

Fitting the doubly differentiated data on the body trajectory with an appropriate function in combination with the diagnostics used yields the same result as an aerodynamic balance but, in contrast to the latter case, the former method is contactless, Fig. 2 shows a typical plot of the acceleration of a particle freely accelerating in a flow behind shock wave. The points in this graph were obtained by double numerical differentiation of the displacement dataset. The fluctuations of the acceleration (and, hence, the fluctuations of the aerodynamic force) at a characteristic frequency of 5×10^3 Hz seem to be related with the separation-zone size pulsations under the unsteady flow regime around particles experiencing an acceleration of $\sim 10^5$ m/sec^2.

2.1. Early stage of flow and free-particle velocity relaxation

The revealed fluctuations of the free-body acceleration in the flow, the fact that the number of available points is usually limited, and problems that arise in numerical differentiation of a function defined, with some experimental error, at a discrete number of points in some cases do not make it possible to find the acceleration with a satisfactory accuracy. For such cases, methods of treating initial datasets or their not-higher-than-first derivatives were developed. This approach yields a new expression for the particle drag in terms of velocity relaxation parameters. The computational part of this algorithm is based on the possibility of fitting the experimental data on particle displacement S_i, known at moments t_i, with some appropriate function $S(t)$. The same approach can be applied to the derivative dataset on particle velocity $V_i = (S_{i+1} - S_i)/(t_{i+1} - t_i)$ to find the value of λ (and, with it, C_x) without measuring the acceleration. The analytical form of the displacement function $S(t)$ and velocity function $V(t)$ for the early stage of velocity relaxation, needed for this procedure, is given below.

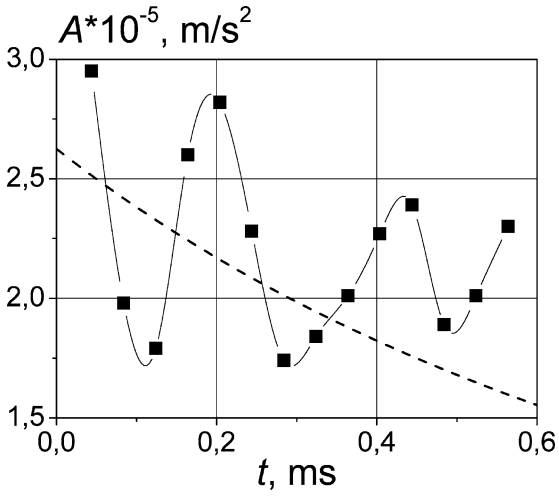

Fig. 2. Acceleration of a particle instantaneously introduced into the flow behind shock wave. The predicted acceleration function (see text) is shown with the dashed line.

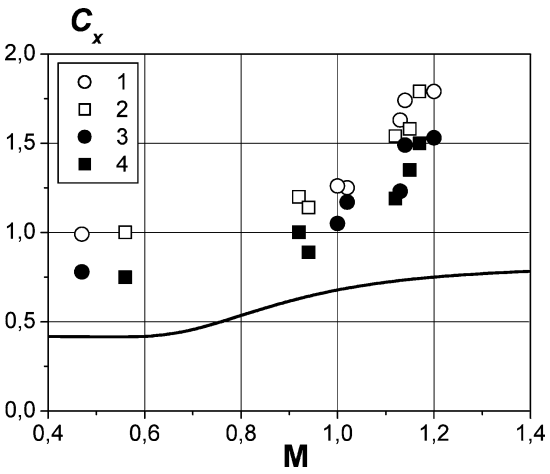

Fig. 3. The drag coefficients C_x of a cube and a sphere in the flow behind shock wave: 1 and 2 – the sphere and the cube whose motion is influenced by the shock-wave front; 3 and 4 – the sphere and the cube not experiencing the action of the shock-wave front; curve – the coefficient C_x of a sphere in a steady-state flow with $Re \sim 10^5$ [1].

At high Reynolds numbers, the equation of motion of a free body instantaneously introduced into a flow has the form $m\frac{\mathrm{d}V}{\mathrm{d}t} = C_x s\frac{\rho(u-V)^2}{2}$ $(V = 0 \text{ at } t = 0)$.

Under an assumption about constancy of C_x, after gathering all fixed parameters in a single parameter

$$\lambda = \frac{2m}{s\rho C_x} \tag{2}$$

the equation of motion reduces to $\frac{\mathrm{d}V}{\mathrm{d}t} = \frac{1}{\lambda}(u - V)^2$ $(V = 0 \text{ at } t = 0)$. This equation is satisfied by the particle velocity function

$$V(t) = u\left(1 - \frac{1}{1 + t/\tau}\right) \quad (\text{where } \tau = \lambda/u) \tag{3}$$

which, after integration and differentiation, gives respectively the displacement function

$$S(t) = \lambda\left[\frac{t}{\tau} - \ln\left(1 + \frac{t}{\tau}\right)\right] \tag{4}$$

and the acceleration function

$$A(t) = \frac{u}{\tau}\frac{1}{(1 + t/\tau)^2} \tag{5}$$

We used functions (3) and (4) to fit the experimental data on particle dynamics at the early stage of velocity relaxation. The values of λ and τ are to be found from the best-fit conditions, using the least squares method or more advanced algorithms. Apparently, if the parameter λ is already known, then the coefficient C_x can be calculated from formula (2):

$$C_x = \frac{2m}{s\rho\lambda} \tag{6}$$

The above formula defines C_x in terms of the velocity relaxation parameters. Formally, definition (6) coincides with (1); together with kinematic functions (3–5), it enables determination of λ not from the body acceleration but as the dimensional coefficient in the displacement function (4). According to the least squares method, in the case of function (4) the sought value of λ (if the velocity u is known) represents a root of the equation

$$\sum_i \left\{ S_i - \left[ut_i - \lambda \ln\left(1 + \frac{u}{\lambda} t_i\right)\right]\right\}\left[\frac{t_i u/\lambda}{1 + (u/\lambda)t_i} - \ln\left(1 + \frac{u}{\lambda} t_i\right)\right] = 0 \tag{7}$$

If the problem involves other unknown parameters (for instance, the flow velocity u), it is possible to obtain and solve a system of similar differential equations involving partial derivatives with respect to corresponding parameters (for instance, with respect to u):

$$\begin{cases} \displaystyle\sum_i^n \big[S_i - S(t_i; u, \lambda)\big] \frac{\partial S(t_i; u, \lambda)}{\partial u} = 0 \\ \displaystyle\sum_i^n \big[S_i - S(t_i; u, \lambda)\big] \frac{\partial S(t_i; u, \lambda)}{\partial \lambda} = 0 \end{cases} \tag{8}$$

Since the particle drag may vary in the course of particle acceleration, the found value of λ should be considered as a time-mean value, as if it was obtained by time averaging over the observation period. The fewer the number of points sampled from the available data array, i.e., the shorter the track of the particle, the more local the measurement is, but less representative is the statistics. Here we observe the indeterminancy inherent to all time-of-flight methods of measuring velocity of moving particles: the higher the spatial resolution of a method, the lower its accuracy. Note, finally, that Eq. (7) has, as a rule, two or more solutions. In some approximation, the true solution can be found considering the physical conditions of the experiment. On the other hand, there exists a more general, totally formal approach, based on dealing exclusively with the experimental data on particle trajectory. This approach is described below.

2.2. Approximate solution

For quick engineering calculations, and also for a preliminary estimation of the domain to which the solution of Eq. (7) falls, we found an approximate analytical formula for the parameter λ. This formula allows one to calculate the coefficient C_x directly from the dataset (S_i, t_i) without solving the transcendent Eq. (7) or a system of equations similar to system (8). This approach is especially useful in solving multi-parametric problems having two or more solutions. Since we consider the early stage of velocity relaxation ($t/\tau < 1$), the following expansion is valid: $\ln(1 + \frac{t}{\tau}) \cong \frac{t}{\tau} - \frac{1}{2}(\frac{t}{\tau})^2 + \frac{1}{3}(\frac{t}{\tau})^3 - \cdots$. Then, we can replace the displacement function (6) with an approximate one,

$$S(t; u, \tau) = \frac{1}{2}\frac{u}{\tau}t^2 - \frac{1}{3}\frac{u}{\tau^2}t^3 + \frac{1}{4}\frac{u}{\tau^3}t^4 - \cdots \tag{9}$$

Introducing new parameters $x_1 = u/2\tau$, $x_2 = u/3\tau^2$, $x_3 = u/4\tau^3, \ldots$, and inserting into (8) the new fitting function $S^*(t; x_1, x_2, \ldots, x_m) = x_1 t^2 - x_2 t^3 + \cdots \pm x_m t^{m+1}$ (here, the signs '+' and '−' should be taken respectively for odd and even m's; $m < n$ is the number of points in the sampled dataset), we obtain a system of m linear equations. We arrive at nothing else than at the problem on finding the coefficients of alternating polynomial (9) with which this polynomial fits the experimental dataset (S_i, t_i) with a minimal root-mean-square

deviation. Not giving here the cumbersome general consideration, we restrict ourselves to presenting, by way of example, the case of two expansion terms:

$$\begin{cases} x_1 \sum_i^n t_i^4 - x_2 \sum_i^n t_i^5 = \sum_i^n S_i t_i^2 \\ x_1 \sum_i^n t_i^5 - x_2 \sum_i^n t_i^6 = \sum_i^n S_i t_i^3 \end{cases}$$

The solution of this system, like that of linear systems of higher orders, can be expressed algebraically through some statistical sums of initial experimental data arrays. For the above system, for instance, we have: $x_1 = (c + bx_2)/a$, $x_2 = (f - bc/a)(b^2/a - e)$ where $a = \sum_i^n t_i^4$, $b = \sum_i^n t_i^5$, $c = \sum_i^n S_i t_i^2$, $e = \sum_i^n t_i^6$, and $f = \sum_i^n S_i t_i^3$; from here, the approximate values of relaxation parameters can be expressed through the polynomial coefficients:

$$\tau^* = \frac{2}{3}\frac{x_1}{x_2}, \qquad \lambda^* = \frac{8}{9}\frac{x_1^3}{x_2^2} \tag{10}$$

If $t_n/\tau^* \ll 1$, then these values can be used as final ones for determining C_x. For example in the experiments in Fig. 1 the observation time is $t_n \sim 0.5$ ms and $\tau \sim 1.3$ ms at the number of the frames $n = 12$–14. Then more members in the alternating polynomial (9) and less frames have to be used for this approach.

2.3. Two-parametric problem

In a number of cases, the flow velocity u is unknown, and there arises a necessity in determining it (or in finding its more accurate value), along with the relaxation parameters, by statistically treating data on particle trajectory. In the above method, the approximate flow velocity u^* is already known since $u^* = \lambda^*/\tau^*$. In a general case, one should solve, instead of Eq. (7), system (8) with some particular displacement function. It is known, however, that, in solving a two-parametric problem, requirements imposed on the accuracy of the initial data array become much more stringent. For this reason, along with the measures to be taken to improve the measurement accuracy, it is generally accepted to use the approach that makes it possible to pass over from solving the two-parametric fitting problem to independent determination of the two parameters explicitly given by algebraic expressions (3)–(5). This approach is based on the fact that each of the sought parameters enters the respective fitting function as a multiplier that can be eliminated by passing over from the data vector F_i to the matrix $F_{ij} = F_i/F_j$, $i < j$. Then, it follows from (3) that the relaxation parameter τ can be independently obtained by statistically treating the dataset formed by the elements of the matrix

$$\tau_{ij} = t_j \frac{1 - V_{ij}}{V_{ij} t_{ji} - 1} \tag{11}$$

where $V_{ij} = V_i/V_j$ and $t_{ji} = t_j/t_i$. Here, V_i is a new dataset to be obtained by numerical differentiation of the initial displacement data array. By eliminating, in a similar manner, the relaxation parameter λ right in the equation of motion and substituting, in this equation, the left-hand side with the numerical value of the acceleration a_i obtained by differentiating the dataset V_i, one can find the flow velocity, averaging the set of elements in the matrix

$$u_{ij} = V_j \frac{\sqrt{a_{ij}} - V_{ij}}{\sqrt{a_{ij}} - 1} \tag{12}$$

where $a_{ij} = a_i/a_j$. Thus, if one wants to determine the relaxation parameters from the initial displacement dataset, then it is necessary to solve the two-parametric approximation problem; from the two derivatives of this dataset, the parameters can be found independently. An important point is that in both cases the proposed approach allows one to obtain, with satisfactory accuracy, an estimate of the relaxation parameter $\lambda = u\tau$ for a given data array S_i

if, for this data array, the inequality $t_n/\tau \ll 1$ is satisfied. Otherwise, if the relaxation time constant τ is comparable with the observation time t_n, then it suffices to use a subset $S_1, \ldots, S_m$ meeting the condition $t_m/\tau \ll 1$. Also, it is of importance that the experimental scheme itself and the physical pattern of the particle interaction with the flow be consistent with the equation of motion (2). A number of problems require using other approaches already at the stage of writing equation of motion and the velocity function deduced from this equation. For a displacement function other than (3), Eq. (7) will acquire a different form, the series expansion (9) and the approximate relaxation parameters (10) deduced from this expansion will no longer be suitable, and the passage from vector data arrays to their matrix representation (11) and (12) will differ from that described above; nevertheless, the above methods will remain in force and ready for application to displacement, velocity, and acceleration functions of any form.

3. Results and discussion

The above methods of treating experimental data on the displacement of free bodies in the flow behind shock waves has allowed us to determine either the mean drag over the whole observation time (in this case, the whole available dataset was used) or the local (drawn from a sampled subset of the initial dataset) drag (b). For instance, points 1 and 2 in Fig. 3 were obtained from the whole data array, including the early stage of velocity relaxation, when the shock-wave front substantially affected the body acceleration; points 3 and 4 in this figure were obtained for a later stage.

For the cube, it is found that there exists its stable orientation with respect to the vector of flow velocity, for which the moment of the aerodynamic force with respect to the center of mass of the cube is zero. This implies that the center of mass of the body and the center of the aerodynamic force either coincide or lie, in the indicated succession, on a straight line coincident with the vector of this force. The cube acquires its stable orientation in a time interval of first 200–400 μsec after the body starts experiencing the action of the flow, and the registered angular velocity the body displays during this process may run into 3000 rpm. The stable orientation of the cube in the flow corresponds to its maximum possible midsection area.

4. Conclusions

For the first time, the multi-frame shadow visualization technique coupled with a laser stroboscopic source of light has been used to obtain data on the dynamics of irregularly shaped bodies freely accelerating in a flow behind shock wave. A fitting procedure for doubly differentiated displacement data array is proposed, which, together with the diagnostic technique used, represents a kind of contactless aerodynamic balance. Data on the drag of spheres and irregularly shaped bodies at the early stage of velocity relaxation in the flow behind shock wave are obtained. The drag of an irregularly shaped body and the drag of a sphere under such conditions are shown to be roughly equal, two to three times exceeding the steady drag of the sphere.

Acknowledgements

This work was supported by the Russian Foundation for Fundamental Research (Grant No. 01-01-00776).

References

[1] V.M. Boiko, V.P. Kiselev, S.P. Kiselev, A.N. Papyrin, S.V. Poplavski, V.M. Fomin, Shock wave interaction with a cloud of particles, Shock Waves 7 (1997) 275–285.